Scientific Research Publishing

Energy and Power Engineering, 2023, 15, 291-306
https://www.scirp.org/journal/epe
ISSN Online: 1947-3818
ISSN Print: 1949-243X

Performance Improvement of CIGS Solar Cell: A Simulation Approach by SCAPS-1D

Md. Ferdous Wahid*, Md. Nuralam Howlader, Nazmul Ahasan, Md. Mizanur Rahman

Department of Electrical and Electronic Engineering, Hajee Mohammad Danesh Science and Technology University, Dinajpur, Bangladesh
Email: *mfwahid26@gmail.com

How to cite this paper: Wahid, M.F., Howlader, M.N., Ahasan, N. and Rahman, M.M. (2023) Performance Improvement of CIGS Solar Cell: A Simulation Approach by SCAPS-1D. *Energy and Power Engineering*, **15**, 291-306.
https://doi.org/10.4236/epe.2023.158015

Received: July 27, 2023
Accepted: August 26, 2023
Published: August 29, 2023

Abstract

Thin-film solar cells possess the distinct advantage of being cost-effective and relatively simple to manufacture. Nevertheless, it is of utmost importance to enhance their overall performance. In this research work, copper indium gallium selenide (CIGS)-based ultra-thin solar cell (SC) configuration (Ag/ZnO/ZnSe/CIGS/Si/Ni) has been designed and examined using SCAPS-1D. The numerical calculations revealed that this new design resulted in a substantial improvement in SC performance. This study explores the utilization of two absorber layers, CIGS and Si, both with a total of 2 μm thickness, to enhance device performance while reducing material costs, observing an increase in key SC parameters as the Si absorber layer thickness is increased, reaching a maximum efficiency of 29.13% when CIGS and Si thicknesses are set at 0.4 μm and 1.6 μm, respectively with doping absorber doping density of 10^{14} cm^{-3}. Furthermore, we analyze the impact of variation in absorber and buffer layer thickness, as well as doping concentration, surface recombination velocity (SRV), electron affinity, series-shunt resistance, and temperature, on optimized CIGS SC parameters such as short-circuit current density (J_{SC}), open circuit voltage (V_{OC}), fill factor (FF), and power conversion efficiency (PCE). The findings yielded by the investigation offer significant elucidation regarding the fabrication of economically viable and highly efficient non-hazardous CIGS ultra-thin SC.

Keywords

Thin-Flim, CIGS-Based Solar Cell, Non-Toxic Solar Cell, SCAPS-1D, Numerical Simulation, Renewable Energy

1. Introduction

Renewable energy sources such as solar energy have the potential to serve as via-

ble alternatives to non-renewable sources, such as fossil fuels. Solar energy, being an in-exhaustible and sustainable energy source, exhibits remarkable potential for meeting energy needs [1]. Notably, solar power generation is not only environmentally friendly, but also free from any adverse consequences such as pollution or noise. Solar cells (SCs) are ingeniously designed to harness the abundant solar energy emitted by the sun and effectively transform it into a readily available form of electrical power. Moreover, SC fabrication has improved greatly over time. However, the cost-effectiveness and overall efficiency of SCs continue to pose significant hurdles in their advancement [2] [3] [4]. Therefore, the primary objective of technological progress in the photovoltaic (PV) sector is to develop high-efficiency SCs while simultaneously minimizing production costs [5] [6] [7]. Hence, throughout the past few decades, extensive research has been conducted by researchers on materials that meet the requirements of affordability, effectiveness, and longevity in the PV field [8] [9]. Copper indium gallium selenide (CIGS), belonging to the group I-III-VI, has emerged as a highly promising choice for thin-film SCs (TFSCs). This is primarily owing to its excellent conversion efficiency, which has recently surpassed 23% [10] [11] [12]. Additionally, CIGS exhibits remarkable stability, cost-effectiveness, and configurable band gap of roughly 1.01 - 1.69 eV [13] [14]. This puts them in close competition with silicon PV cells, which currently have a PCE of 26.7% [15] and other competing materials such as a-Si, CdTe [16] and CZTS [17]. Moreover, it has an excellent absorption coefficient in the visual spectrum of approximately 10^5 cm^{-1}, making it more desirable and effective for solar applications [6] [10]. However, the challenge lies in the fact that the combination of Ga (Gallium) and In (Indium) materials in the CIGS sample is both scarce and expensive. As a result, researchers are directing their attention towards reducing the thickness of the absorber layer to minimize the usage of Gallium and indium in an effort to decrease the overall production expenses. But, the electrical properties of CIGS TFSCs are influenced by the thickness of the active layer, and a reduction in thickness can potentially lower SC performance. The ideal thickness of the active layer, according to some researchers, is between 2 and 3 μm [18] [19]. On the other hand, recent studies have produced CIGS-based cells having active layer thicknesses of under 1 μm that are quite effective [20]-[24]. In a study conducted by Movla *et al*. [20], it was shown that an absorber layer made of graded CIGS material with a thickness of 0.5 μm, combined with a transparent conductive oxide (TCO) layer of thickness 20 nm, results in an impressive efficiency of 20.34%. Similarly, Vermang *et al*. carried out a study where they achieved an efficiency of up to 13.5% using ultra-thin CIGS solar cells [21]. These cells had a CIGS absorber layer with a thickness of 0.385 μm. The experimental PV solar cell efficiencies were investigated by Garris *et al*. [22] over a range of thicknesses. They discovered a remarkable efficiency of 15.15% in a CIGS layer with a thickness of 0.490 μm. In a separate investigation carried out by Chadel *et al*. [23], an impressive conversion efficiency of 24.43% was attained by utilizing a 0.2 μm CIGS absorber layer in con-

junction with a 1 μm Si BSF layer. The results of earlier studies offer useful information for optimizing ultra-thin CIGS solar cells, resulting in increased efficiency and stability with reduced cost. Therefore, in order to develop a low-cost CIGS solar cell with enhanced efficiency, we introduced a dual absorber layer-based SC.

In this paper, an alternative configuration of CIGS-based ultra-thin SC has been proposed. The numerical analysis of the performance of a newly proposed Ag/ZnO/ZnSe/CIGS/Si/Ni SC is conducted using the SCAPS-1D simulator. SCAPS-1D has gained extensive popularity for numerical simulations of SC due to its open-source characteristics, adaptability, ease of use, and precision. Here, we employed a dual absorber configuration consisting of two distinct layers, namely CIGS and Si. A SC with two absorber layers is more effective because it can absorb solar photons throughout a wider spectral range [25]. To get maximum performance at the lowest cost, we put a specific emphasis on optimizing the thickness of the absorber layer. Moreover, cadmium sulphide (CdS) is commonly employed as a buffer layer in CIGS SCs. The toxicity of cadmium is the most significant disadvantage of CdS. Hence, in order to develop an environmentally friendly and non-toxic CIGS SC, CdS buffer layer is substituted with a ZnSe layer, and the optimization process is subsequently pursued. Furthermore, we investigate the impact of incorporating a Si absorber layer on the performance of the device. In addition, we explore the effects of changes in the thickness of the absorber and buffer layers, as well as variations in doping concentration, surface recombination velocity (SRV), electron affinity, series-shunt resistance and temperature, on the optimized CIGS SC parameters.

2. Device Configuration and Material Parameters

The investigation of performance parameters for the newly designed Ag/ZnO/ZnSe/CIGS/Si/Ni SC involved the use of one-dimensional electrical Solar Cell Capacitance Simulator structures (SCAPS-1D) software. This software developed by the Department of Electronics and Information Systems at the University of Ghent, Belgium, analyzed the electrostatic potential and behaviour of free carriers within the SC through the implementation of the continuity equations and Poisson equation, comprising up to seven semiconductor materials [26]. The device configuration of the newly developed SC is shown in **Figure 1(a)**. The SC is made up of a p-CIGS and p-Si absorber layer, an n-ZnO window layer, and an n-ZnSe buffer layer. The additional p-Si absorber layer in the proposed design has a band gap of 1.12 eV. To facilitate efficient light absorption, minimize electrical losses, promote effective charge carrier transfer, and protect the underlying layers, we employ ZnO as window layer. ZnO is preferred due to its high transparency, low resistivity, favorable interface characteristics, and wide bandgap. ZnSe serves as the buffer layer due to its non-toxicity, high optical transmittance, and wide bandgap, which together contribute to a substantial optical throughput in the hetero-junction structure. The suitable electron affinity of the ZnSe buffer

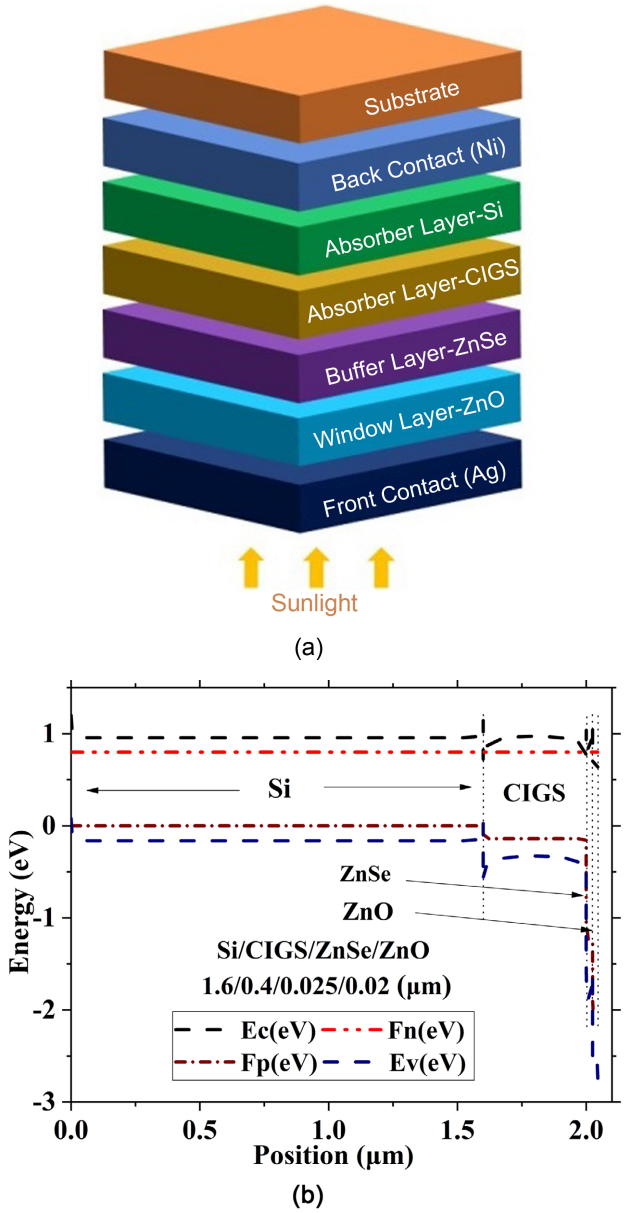

Figure 1. (a) Newly developed CIGS SC configuration; (b) Energy band diagram.

layer enables the formation of an appropriate junction with CIGS. Moreover, the introduction of the p-Si absorber layer exhibits favorable band alignment with CIGS, leading to enhanced light absorption. The energy band diagram of the proposed SC structure is presented in **Figure 1(b)**. For the front and rear contacts, Ag and Ni are employed, respectively. A working temperature of 300 K is used for all simulations, with AM 1.5G light. This study utilizes previous research efforts on experimentally and theoretically determined parameters of different layers, as described in various research papers, to enhance the performance of the newly developed CIGS solar cell. The relevant physical parameters for each layer are outlined in **Table 1** and **Table 2**.

Table 1. Physical parameters of various layers from literature.

Parameter	p-Si [27]	n-ZnO [27]	p-CIGS [27]	n-ZnSe [28]
Thickness (μm)	1.6	0.02	0.4	0.025
Electron Affinity, χ_e (ev)	4.05	4.60	4.50	4.09
Dielectric Constant, ϵ_r	11.90	9	13.60	10
Bandgap (ev)	1.12	3.30	1.30	2.700
Density of States in Conduction Band (cm^{-3})	2.2×10^{19}	2.2×10^{18}	2.2×10^{18}	2.2×10^{18}
Density of States in Valence Band (cm^{-3})	2.65×10^{19}	1.8×10^{18}	1.8×10^{18}	1.8×10^{19}
Electron Mobility, μp (cm^2/V-Sec)	1400	100	100	50
Hole Mobility, μn (cm^2/V-Sec)	500	25	25	20
Donor Density, Nd (cm^{-3})	0	1×10^{20}	0	2×10^{18}
Acceptor Density, Na (cm^{-3})	1×10^{14}	0	2×10^{14}	0

Table 2. Contact properties from literature [29].

Parameters	Back Contact (Ni)	Front Contact (Ag)
Electron SRV (cms^{-1})	10^5	10^7
Hole SRV (cms^{-1})	10^7	10^5
Work Function (eV)	5.25	4.26

3. Result and Discussion

3.1. Impact of Absorber Layer Thickness

The thickness of the absorber layer plays a pivotal role in the development of SC. This is due to the fact that a thicker absorber layer can lead to an increase in carrier recombination, while a thinner absorber layer may result in insufficient light ab-sorption [25]. Consequently, the current density and efficiency of the SC experience a decrease. Therefore, it is essential to meticulously choose the appropriate thickness in order to enhance the performance of the SC.

As can be seen in **Figure 2**, the V_{OC}, J_{SC}, FF, and PCE are all influenced by the absorber layer thickness. When the CIGS/Si is thickened, more pairs of electrons and holes are produced, which advances efficiency and causes a decrease in FF owing to resistance and an increase in J_{SC}. The symbols (C1 to C11) are used to indicate the thickness combinations among the two absorber layers, which are demonstrated in **Table 3**. It is observed from **Figure 2** that maximum SC performance has been achieved with thickness combination C9, where CIGS of 0.4 μm and Si of 1.6 μm thicknesses were used. This demonstrated that an increase in the thickness of the Si layer leads to an increase in SC performance.

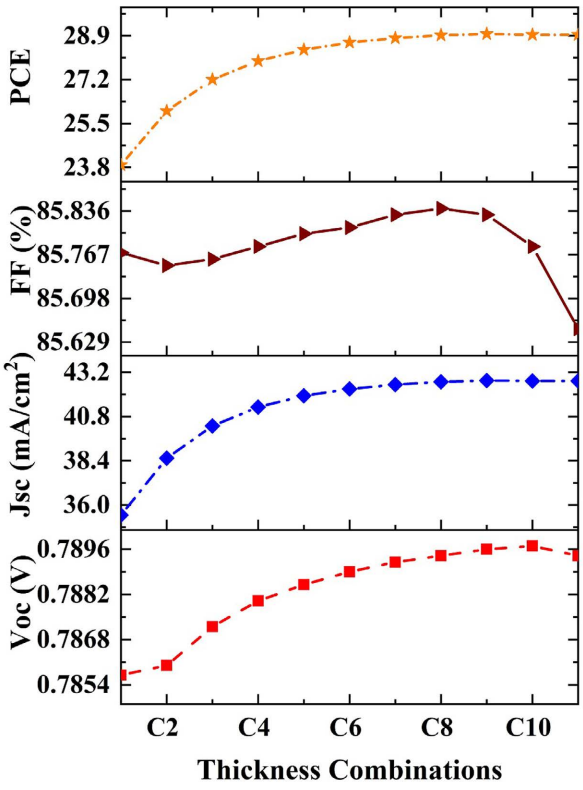

Figure 2. Impact of varied thicknesses of CIGS and Si absorber layers on Voc, Jsc, FF and PCE.

Table 3. Thickness combination of CIGS and Si in absorber layer.

Thickness (μm) Combination	C1	C2	C3	C4	C5	C6	C7	C8	C9	C10	C11
CIGS	2	1.8	1.6	1.4	1.2	1	0.8	0.6	0.4	0.2	0
Si	0	0.2	0.4	0.6	0.8	1	1.2	1.4	1.6	1.8	2

3.2. Doping Concentration Optimization of CIGS and Si Layer

The influence of doping concentration on the performance of SCs was studied by examining the impact of changing the doping concentration from 10^{12} to 10^{20} cm^{-3} in the CIGS and Si absorber layers, while maintaining the respective layer thicknesses at 0.4 and 1.6 μm, as depicted in **Figure 3(a)** and **Figure 3(b)**. The SC output characteristics barely change when the CIGS absorber layer and Si layer's doping concentration changes 10^{12} to 10^{16} cm^{-3}. Beyond the doping concentration of 10^{16} cm^{-3} of the CIGS absorber layer and Si layer, the value of V_{OC} rises. Doping changes the Fermi level within the semiconductor, bringing it closer to the energy level of the bandgap. As a result, the built-in potential rises, raising the V_{OC} [30]. The value of Jsc decreases with the increase in doping concentration of the both absorber layer. This is due to the increase in carrier recombination at higher doping densities [31]. The FF and PCE also show the similar down trend beyond doping concentration 10^{16} cm^{-3} for both absorber layers.

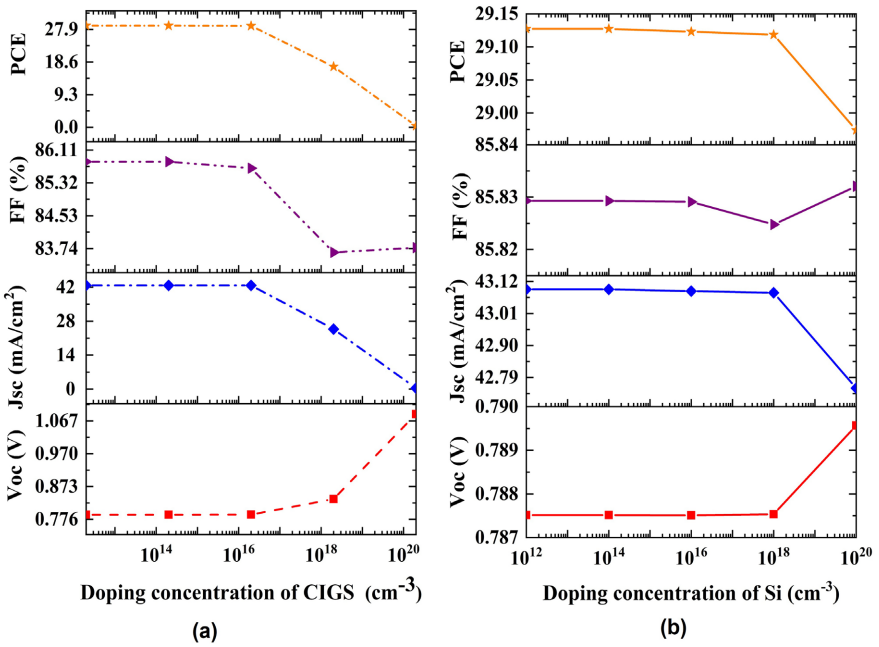

Figure 3. Variation of performance parameters for doping concentration of CIGS and Si absorber layer.

The findings demonstrate that the optimal performance of the newly developed dual absorber CIGS-based SC has obtained with the doping concentration of 10^{14} cm^{-3} which yield overall PCE of 29.13%.

3.3. Effect of Thickness and Doping Concentration of ZnSe Buffer Layer on SC Parameters

The thickness and doping concentration of the ZnSe buffer layer have been optimized by varying them from 0.02 μm to 0.4 μm and 10^{12} to 10^{20} cm^{-3} correspondingly. The result is illustrated in **Figure 4**. **Figure 4** depicts the SCs influence on Voc, with the values rising slightly in accordance with the thickness of the ZnSe buffer layer. Additionally, it has been shown that the Jsc values of the SC decrease as the thickness of the ZnSe buffer layer increases. This is due to the fact that a larger buffer layer leads to more photon losses [32]. Consequently, it would result in a reduction in the number of photons that passed through the absorber layer. When the ZnSe buffer layer is thicker, the FF and PCE also begin to decline. Jsc, FF, and PCE, which are at their greatest levels at lower doping concentrations except Voc. Voc is not significantly affected by variations in the doping concentration of the ZnSe buffer layer. However, increased buffer layer doping concentration creates a powerful electric field that efficiently attracts electrons and opposes minority carriers away from the interface between the buffer layer and absorber layer, reducing interface recombination [32]. We choose the thickness 0.025 μm and doping concentration 10^{18} cm^{-3} at which the Voc, Jsc, FF, and PCE are 0.7875 V, 43.0927 mA/cm^2, 85.83%, and 29.13%, respectively, taking into consideration of fabrication cost and SC's performances.

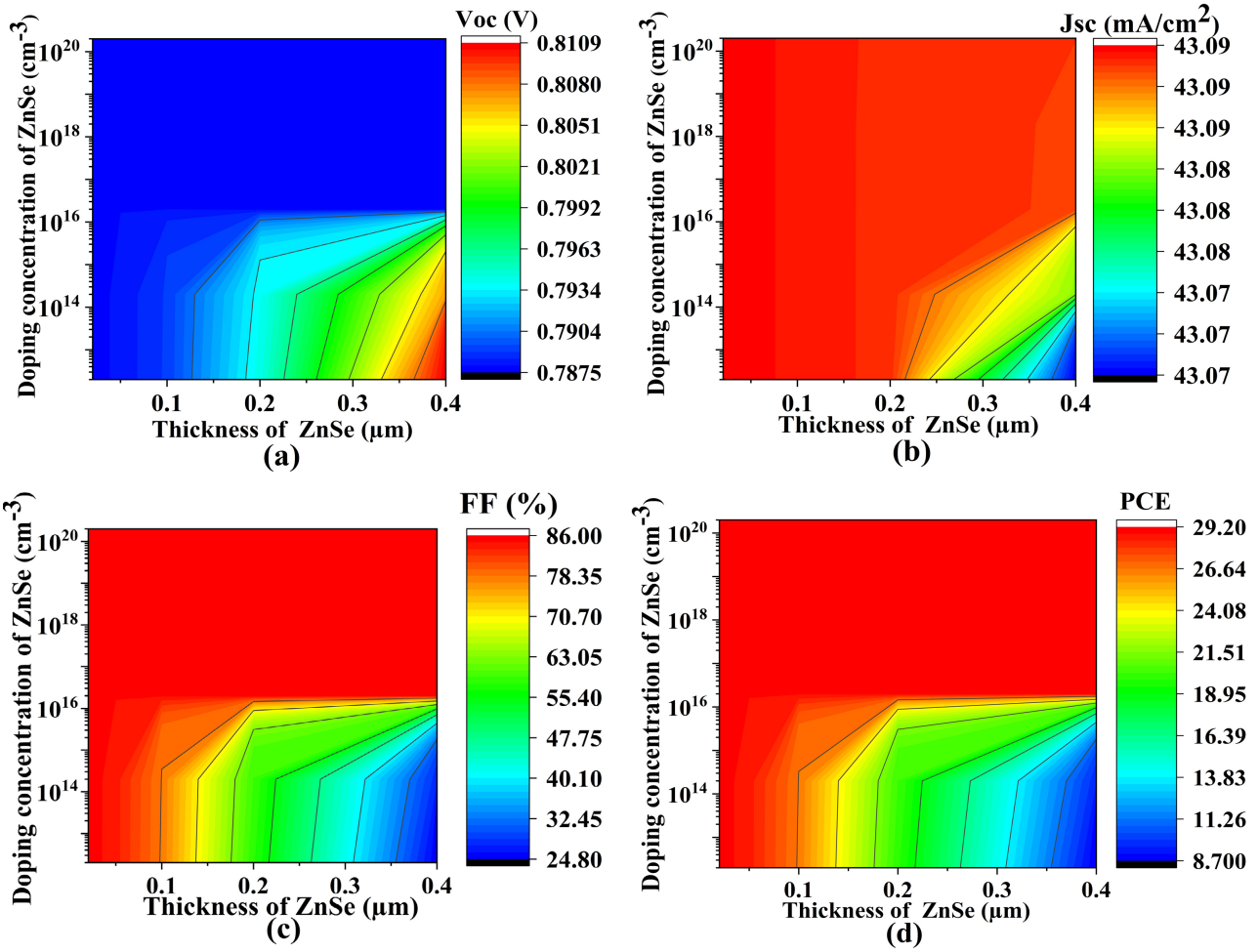

Figure 4. Variation of performance parameters for thickness and doping concentration of ZnSe buffer layer.

3.4. Impact of Series and Shunt Resistance on CIGS-Based Solar Cell

Figure 5 illustrates the assessment of PV characteristics by changing the series resistance from 1 to 5 ohm-cm^2 and the shunt resistance from 10 to 10^5 ohm-cm^2. A slight variation in Voc is observed due to changes in the series and shunt resistance, with Voc changing from 0.43 V to 0.78 V only when the shunt resistance ranges from 10 to 10^2 ohm-cm^2, after which it remains relatively constant. Moreover, Figure 5 indicates a significant variation in the value of Jsc, showing an increase when the series resistance is low and the shunt resistance is high, leading to a significant improvement in Jsc of 39.17 mA/cm^2 to 43.09 mA/cm^2 for shunt resistance values between 1 and 10^5 ohm-cm^2 and a decrease of 39.17 mA/cm^2 to 28.72 mA/cm^2 for series resistance values between 1 and 5 ohm-cm^2. It is noticed from Figure 5 that the impact of series resistance on FF and PCE is minimal, while shunt resistance shows a significant effect on FF and PCE, leading to an increase in both FF and PCE from 25.00% to 80.64% and 4.22% to 27.40%, respectively, as the shunt resistance value increases from 1 to 10^5 ohm-cm^2.

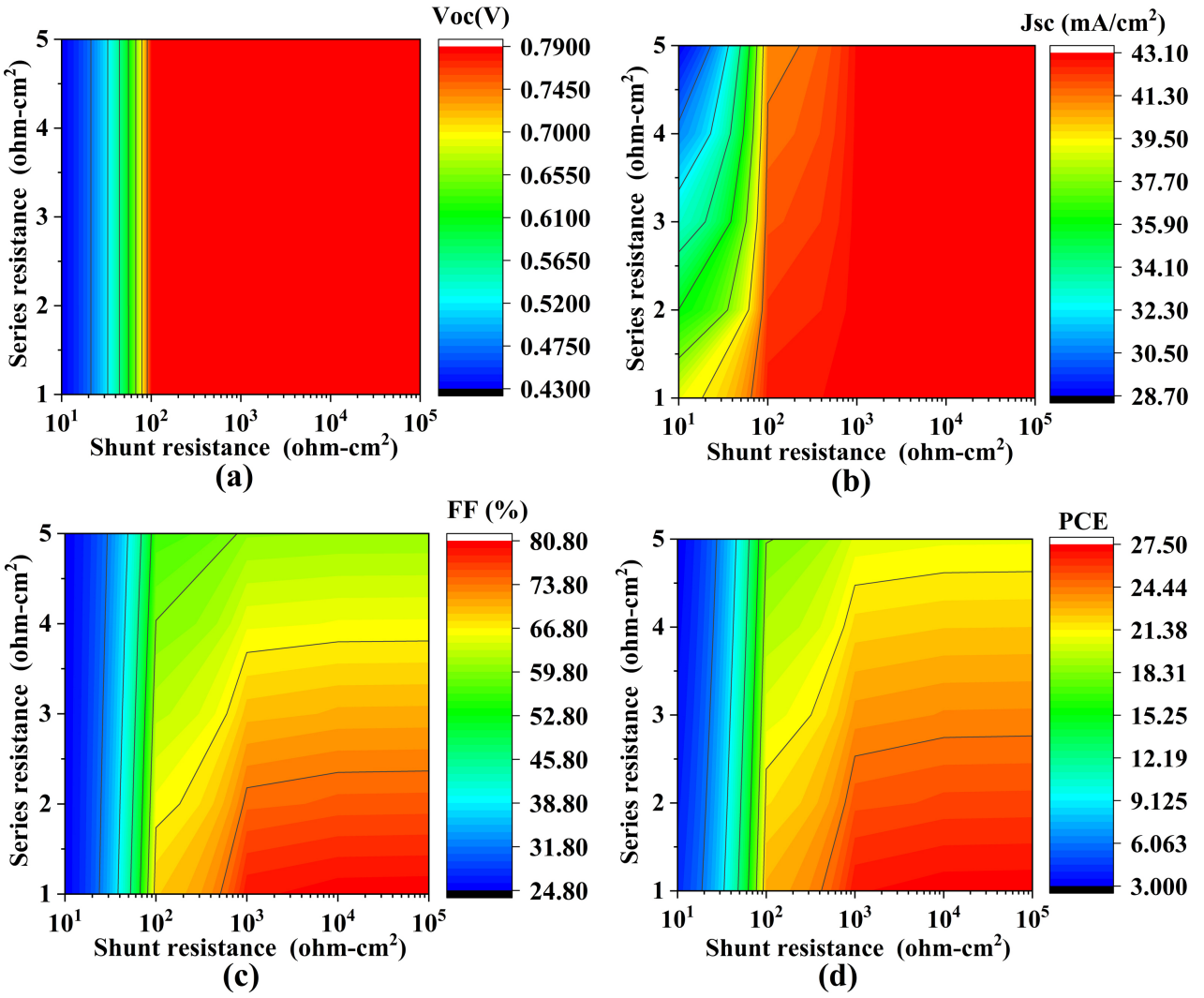

Figure 5. The impact of series and shunt resistance on SC parameters.

3.5. Variation of Parameters Due to Electron Affinity

The influence of the electron affinity of the CIGS absorber layer on the properties of the SC is shown in **Figure 6**. When the electron affinity of absorber layer fluctuates between 4.1 and 4.6 eV, Voc and Jsc values raise. At the interface between the semiconductor material and the absorber layer, a stronger electron affinity encourages more effective charge separation, which increases the flow of electrons [10]. The FF and PCE, however, decrease as the electron affinity value increases over 4.4 eV. This may be related to the SC's rising resistance.

3.6. Impact of Surface Recombination Velocity on SC Parameters

In thinner absorber layers, the proximity between the back contact and depletion region is significantly reduced, thereby enhancing the likelihood of carrier recombination in the back contact. This indicates the importance of investigating the impact of surface recombination velocity (SRV) on the performance of SC parameters. The impact of the SRV varying from 10^2 to 10^8 cms^{-1} has been studied

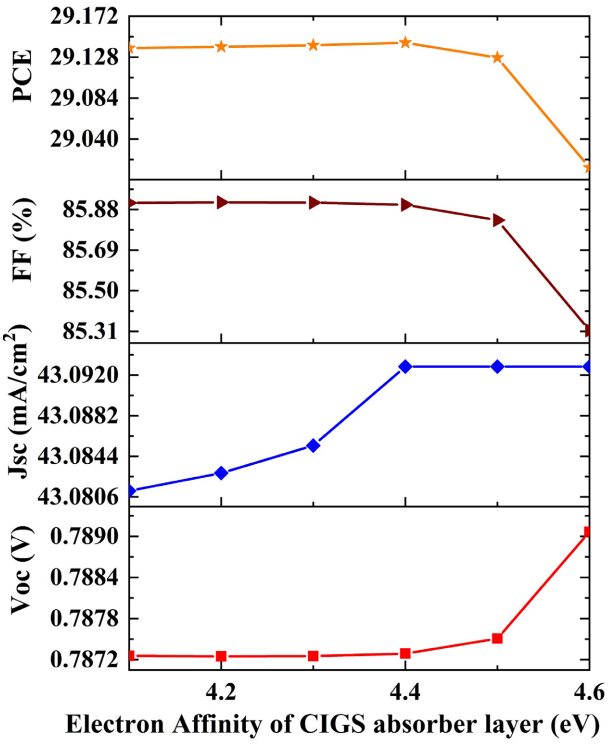

Figure 6. The impact of varying electron affinity of CIGS on SC parameters.

and is depicted in Figure 7. It is observed that Voc of 0.96 V at 10^2 cms^{-1} and deteriorates till 0.61 V with decreasing of SRV till 10^5 cms^{-1}. But the curve of Jsc is 43.09 mA/cm^2, which is constant with respect to increasing SRV. FF is gradually decreased until it reaches 10^6 cms^{-1}, after that point it is abruptly decreased. The surface recombination velocity impacts the efficiency by decreasing a constant manner. Due to the rapid recombination of electrons and holes, a high SRV drastically reduces the minority carrier lifetime and diffusion length, thereby decreasing the SC performance parameters [33]. A fixed value is always chosen for perfect SRV. At 10^5 cms^{-1} SRV, We get the value of Voc, Jsc, FF, and PCE are 0.78 V, 43.09 mA/cm^2, 85.83%, and 29.12%, respectively.

3.7. Variation of CIGS Output Parameters Due to Temperature

The assessment of the Voc, Jsc, FF, and PCE has been carried out to evaluate the implications of the temperature change between 280 K and 380 K, as depicted in Figure 8. For the proposed CIGS-based hetero-structure, Voc, FF, and PCE values have changed from 0.81 V to 0.66 V, 86.81% to 81.01%, and 30.60% to 23.25%, respectively, between 280 K and 380 K. However, Jsc is 43.09 mA/cm^2, which remains unchanged. It has been noticed that temperature change considerably deteriorates the values of Voc, FF, and PCE in the hetero-structures as a consequence of temperature-induced shrinking of the band gap [34]. But nonetheless, Jsc in the hetero-structures remains stable, indicating that the creation of electron-hole pairs and the recombination are consistent throughout the entire

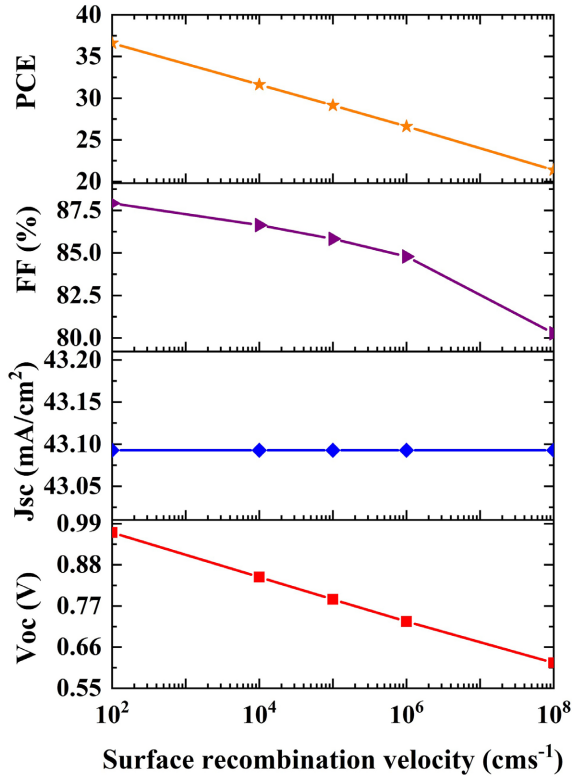

Figure 7. The impact of surface recombination velocity on SC parameters.

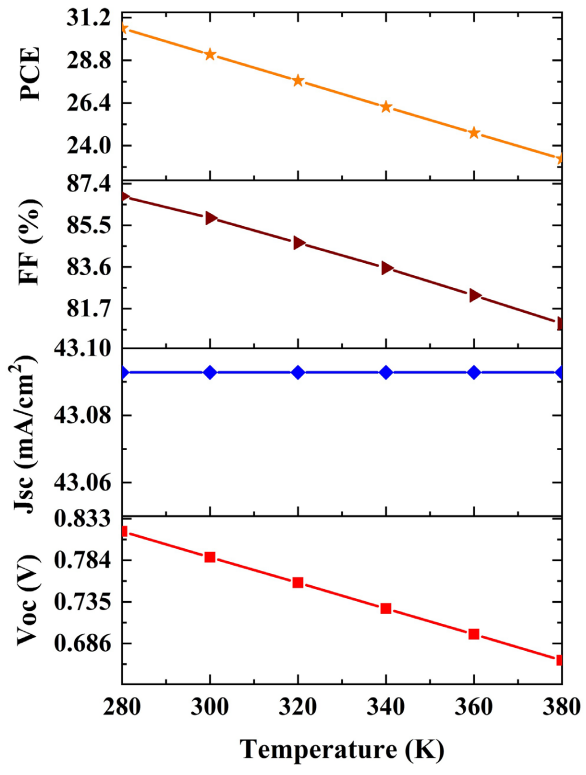

Figure 8. The impact of temperature on SC parameters.

temperature range [35].

3.8. I-V Curve and Quantum Efficiency (QE) of the Newly Designed SC

Figure 9(b) demonstrates the QE of the Ag/ZnO/ZnSe/CIGS/Si/Ni structure using AM1.5 illumination. Since CIGS absorber layer absorbs light of intermediate wavelength ranging from 300 nm to 1100 nm, Q.E. is large in that region [36]. Due to the device producing greater electron-hole pairs as a consequence of the strong absorption, the current density rises. In addition, QE declines in the broad wavelength region from 1100 and 1200 nm. The most probable cause of the condition is insufficient long-wavelength photon absorption [10].

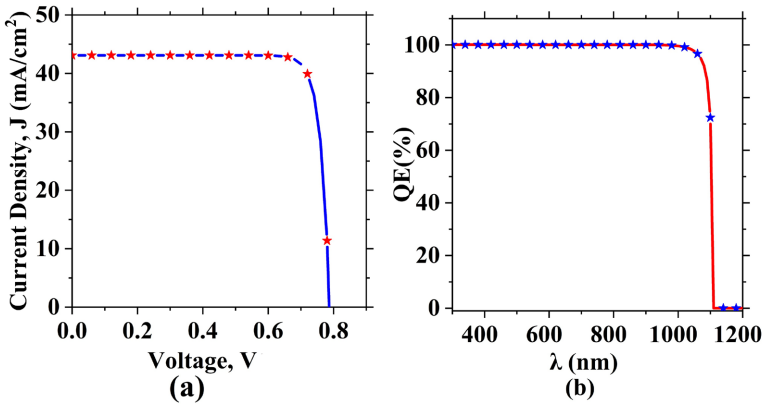

Figure 9. (a) I-V curve; (b) Quantum efficiency (QE) curve.

Table 4. Comparative analysis.

Work Category	Absorber Layer	Buffer Layer	PCE (%)	References
Experimental	CIGS	CdS	15.6	[12]
Simulation	CIGS	CdS	13.08	[6]
Simulation	CIGS	ZnMgO/Zn(O,S)	17.67	[9]
Simulation	CIGS	CdS	21.3	[5]
Simulation	CIGS	CdS	24.22	[10]
Simulation	CIGS	CdS	25.05	[14]
Simulation	CIGS	CdS	26	[11]
Simulation	CIGS	ZnS	26.30	[37]
Simulation	CIGS	ZnMgO/Zn(O,S)	27.3	[9]
Simulation	CIGS	CdS	28.08	[7]
Simulation	CIGS	CdS	18.15	[38]
Simulation	CIGS	InP	28.01	[30]
Simulation	CIGS/Si	ZnSe	29.13	This Research

3.9. Comparative Analysis

In this study, the advantage of incorporating absorber (Si) layer into CIGS-based TFSCs using ZnSe as a buffer layer has been investigated. A Si absorber layer of 1.6 μm and a buffer layer of 0.025 μm, in addition to the CIGS absorber layer, contribute to the overall 29.13% efficiency in this SC, which is higher than the reported CIGS SC in previous studies, listed in **Table 4**. The addition of this absorber layer greatly increases the performance of the SC.

4. Conclusion

CIGS-based SC configuration of Ag/ZnO/ZnSe/CIGS/Si/Ni was proposed and simulated using SCAPS-1D software, and numerical calculations revealed that this new design resulted in a substantial improvement in SC performance. This study explores the utilization of two absorber layers, CIGS and Si, both with a total of 2 μm thickness, to enhance device performance while reducing material costs, observing an increase in key SC parameters as the Si absorber layer thickness is increased, reaching a maximum efficiency of 29.13% when CIGS and Si thicknesses are set at 0.4 μm and 1.6 μm, respectively with doping absorber doping density of 10^{14} cm^{-3}. The output parameters have been meticulously determined through a comprehensive analysis of the effect of buffer layer thickness variation and doping concentration variation, SRV, series-shunt resistance, and temperature. The incorporation of the silicon (Si) layer boosts the absorption of photons and decreases the recombination rate, thereby ultimately leading to enhanced output efficiency parameters. The aforementioned findings indicate that the recently developed SC configuration holds great promise for integration within the solar cell community, enabling the realization of highly efficient CIGS SCs while simultaneously reducing overall costs.

Acknowledgements

The University of Gent's Prof. Marc Burgelman and his colleagues kindly provided the SCAPS-1D software that is discussed in this article, and the authors are appreciative of their assistance.

Conflicts of Interest

The authors declare no conflicts of interest regarding the publication of this paper.

References

[1] Chen, J. (2017) An Empirical Study on China's Energy Supply-and-Demand Model Considering Carbon Emission Peak Constraints in 2030. *Engineering*, **3**, 512-517. https://doi.org/10.1016/J.ENG.2017.04.019

[2] Powalla, M., Paetel, S., Hariskos, D., Wuerz, R., Kessler, F., Lechner, P., *et al.* (2017) Advances in Cost-Efficient Thin-Film Photovoltaics Based on Cu (In, Ga) Se_2. *Engineering*, **3**, 445-451. https://doi.org/10.1016/J.ENG.2017.04.015

[3] Sara, B., Baya, Z. and Zineb, B. (2018) Investigation of Cu (In, Ga) Se_2 Solar Cell Performance with Non-Cadmium Buffer Layer Using TCAD-SILVACO. *Materials Science-Poland*, **36**, 514-519. https://doi.org/10.2478/msp-2018-0054

[4] Dabbabi, S., Nasr, T.B. and Kamoun-Turki, N. (2017) Parameters Optimization of CIGS Solar Cell Using 2D Physical Modeling. *Results in Physics*, **7**, 4020-4024. https://doi.org/10.1016/j.rinp.2017.06.057

[5] Heriche, H., Rouabah, Z. and Bouarissa, N. (2017) New Ultra-Thin CIGS Structure Solar Cells Using SCAPS Simulation Program. *International Journal of Hydrogen Energy*, **42**, 9524-9532. https://doi.org/10.1016/j.ijhydene.2017.02.099

[6] Boukortt, N.E.I., Patanè, S., Adouane, M. and AlHammadi, R. (2021) Numerical Optimization of Ultrathin CIGS Solar Cells with Rear Surface Passivation. *Solar Energy*, **220**, 590-597. https://doi.org/10.1016/j.solener.2021.03.078

[7] Ait Abdelkadir, A., Oublal, E., Sahal, M., Soucase, B.M., Kotri, A., Hangoure, M., *et al*. (2023) Numerical Simulation and Optimization of n-Al-ZnO/n-CdS/p-CIGS/p-Si/p-MoOx/Mo Tandem Solar Cell. *Silicon*, **15**, 2125-2135. https://doi.org/10.1007/s12633-022-02144-1

[8] Benbouzid, Z., Benstaali, W., Rahal, W.L., Hassini, N., Benzidane, M.R. and Boukortt, A. (2023) Efficiency Enhancement by BSF Optimization on Cu (In_{1-x}, Ga_x) Se_2 Solar Cells with Tin (IV) Sulfide Buffer Layer. *Journal of Electronic Materials*, **52**, 4575-4586. https://doi.org/10.1007/s11664-023-10416-8

[9] Gharibshahian, I., Orouji, A.A. and Sharbati, S. (2022) Effectiveness of Band Discontinuities between CIGS Absorber and Copper-Based Hole Transport Layer in Limiting Recombination at the Back Contact. *Materials Today Communications*, **33**, Article ID: 104220. https://doi.org/10.1016/j.mtcomm.2022.104220

[10] Barman, B. and Kalita, P.K. (2021) Influence of Back Surface Field Layer on Enhancing the Efficiency of CIGS Solar Cell. *Solar Energy*, **216**, 329-337. https://doi.org/10.1016/j.solener.2021.01.032

[11] Mohottige, R.N. and Vithanage, S.P.K. (2021) Numerical Simulation of a New Device Architecture for CIGS-Based Thin-Film Solar Cells Using 1D-SCAPS Simulator. *Journal of Photochemistry and Photobiology A*: *Chemistry*, **407**, Article ID: 113079. https://doi.org/10.1016/j.jphotochem.2020.113079

[12] Ghamsari-Yazdel, F. and Fattah, A. (2022) Performance Enhancement of CIGS Solar Cells Using ITO as Buffer Layer. *Micro and Nanostructures*, **168**, Article ID: 207289. https://doi.org/10.1016/j.micrna.2022.207289

[13] Hedayati, M., Olyaee, S. and Ghorashi, S.M.B. (2020) The Effect of Adsorbent Layer Thickness and Gallium Concentration on the Efficiency of a Dual-Junction Copper Indium Gallium Diselenide Solar Cell. *Journal of Electronic Materials*, **49**, 1454-1461. https://doi.org/10.1007/s11664-019-07824-0

[14] Boukortt, N.E.I., Patanè, S. and Abdulraheem, Y.M. (2020) Numerical Investigation of CIGS Thin-Film Solar Cells. *Solar Energy*, **204**, 440-447. https://doi.org/10.1016/j.solener.2020.05.021

[15] Yoshikawa, K., Kawasaki, H., Yoshida, W., Irie, T., Konishi, K., Nakano, K., *et al*. (2017) Silicon Heterojunction Solar Cell with Interdigitated Back Contacts for a Photoconversion Efficiency over 26%. *Nature Energy*, **2**, Article No. 17032. https://doi.org/10.1038/nenergy.2017.32

[16] Kazmi, S.A.A., Khan, A.D., Khan, A.D., Rauf, A., Farooq, W., Noman, M., *et al*. (2020) Efficient Materials for Thin-Film CdTe Solar Cell Based on Back Surface Field and Distributed Bragg Reflector. *Applied Physics A*, **126**, Article No. 46. https://doi.org/10.1007/s00339-019-3221-5

[17] Haghighi, M., Minbashi, M., Taghavinia, N., Kim, D.H., Mahdavi, S.M. and Kordbacheh, A.A. (2018) A Modeling Study on Utilizing SnS_2 as the Buffer Layer of CZT (S, Se) Solar Cells. *Solar Energy*, **167**, 165-171. https://doi.org/10.1016/j.solener.2018.04.010

[18] Pettersson, J., Törndahl, T., Platzer-Björkman, C., Hultqvist, A. and Edoff, M. (2013) The Influence of Absorber Thickness on Cu (In, Ga) Se Solar Cells with Different Buffer Layers. *IEEE Journal of Photovoltaics*, **3**, 1376-1382. https://doi.org/10.1109/JPHOTOV.2013.2276030

[19] Asma, C., Boumdienne, B. and Meriem, C. (2016) Numerical Analysis of the Effect Graded Zn (O, S) on the Performance of the Graded CIGS Based Solar Cells by SCAPS-1D. *International Journal of Nanoelectronics and Materials*, **9**, 103-110.

[20] Movla, H., Abdi, E. and Salami, D. (2013) Simulation Analysis of the CIGS Based Thin Film Solar Cells. *Optik*, **124**, 5871-5873. https://doi.org/10.1016/j.ijleo.2013.04.064

[21] Vermang, B., Wätjen, J.T., Fjällström, V., Rostvall, F., Edoff, M., Kotipalli, R., *et al*. (2014) Employing Si Solar Cell Technology to Increase Efficiency of Ultra-Thin Cu (In, Ga) Se_2 Solar Cells. *Progress in Photovoltaics*: *Research and Applications*, **22**, 1023-1029. https://doi.org/10.1002/pip.2527

[22] Garris, R.L., Johnston, S., Li, J.V., Guthrey, H.L., Ramanathan, K. and Mansfield, L.M. (2018) Electrical Characterization and Comparison of CIGS Solar Cells Made with Different Structures and Fabrication Techniques. *Solar Energy Materials and Solar Cells*, **174**, 77-83. https://doi.org/10.1016/j.solmat.2017.08.027

[23] Chadel, M., Chadel, A., Benyoucef, B. and Aillerie, M. (2023) Enhancement in Efficiency of CIGS Solar Cell by Using a p-Si BSF Layer. *Energies*, **16**, Article 2956. https://doi.org/10.3390/en16072956

[24] Ahamed, E.I., Bhowmik, S., Matin, M.A. and Amin, N. (2017) Highly Efficient Ultra-Thin Cu(In, Ga)Se_2 Solar Cell with Tin Selenide BSF. 2017 *International Conference on Electrical*, *Computer and Communication Engineering (ECCE)*, Cox's Bazar, 16-18 February 2017, 428-432. https://doi.org/10.1109/ECACE.2017.7912942

[25] Maurya, K.K. and Singh, V.N. (2022) Sb_2Se_3/CZTS Dual Absorber Layer Based Solar Cell with 36.32% Efficiency: A Numerical Simulation. *Journal of Science*: *Advanced Materials and Devices*, **7**, Article ID: 100445. https://doi.org/10.1016/j.jsamd.2022.100445

[26] Burgelman, M. and Marlein, J. (2008) Analysis of Graded Band Gap Solar Cells with SCAPS. 23*rd European Photovoltaic Solar Energy Conference*, Valencia, 1-5 September 2008, 2151-2155.

[27] Alam, U. and Sahu, A. (2020) Improved Performance of Ultra-Thin CIGS Structure with ZnS Buffer Layers. 2020 *International Conference on Electrical and Electronics Engineering* (*ICE*3), Gorakhpur, 14-15 February 2020, 534-537. https://doi.org/10.1109/ICE348803.2020.9122990

[28] Hossain, J. (2021) Design and Simulation of Double-Heterojunction Solar Cells Based on Si and GaAs Wafers. *Journal of Physics Communications*, **5**, Article ID: 085008. https://doi.org/10.1088/2399-6528/ac1bc0

[29] Kumar, A. and Thakur, A.D. (2018) Role of Contact Work Function, Back Surface Field, and Conduction Band Offset in Cu_2ZnSnS_4 Solar Cell. *Japanese Journal of Applied Physics*, **57**, Article ID: 08RC05. https://doi.org/10.7567/JJAP.57.08RC05

[30] Deo, M. and Chauhan, R.K. (2023) Tweaking the Performance of Thin Film CIGS Solar Cell Using InP as Buffer Layer. *Optik*, **273**, Article ID: 170357. https://doi.org/10.1016/j.ijleo.2022.170357

[31] Tobbeche, S., Kalache, S., Elbar, M., Kateb, M.N. and Serdouk, M.R. (2019) Improvement of the CIGS Solar Cell Performance: Structure Based on a ZnS buFfer Layer. *Optical and Quantum Electronics*, **51**, Article No. 284. https://doi.org/10.1007/s11082-019-2000-z

[32] Mostefaoui, M., Mazari, H., Khelifi, S., Bouraiou, A. and Dabou, R. (2015) Simulation of High Efficiency CIGS Solar Cells with SCAPS-1D Software. *Energy Procedia*, **74**, 736-744. https://doi.org/10.1016/j.egypro.2015.07.809

[33] Ali, K., Khan, H.M., Anmol, M., Ahmad, I.A., Farooq, W.A., Al-Asbahi, B.A., *et al*. (2020) Effect of Surface Recombination Velocity (SRV) on the Efficiency of Silicon Solar Cell. *Journal of Optoelectronics and Advanced Materials*, **22**, 251-255.

[34] Khatun, M.M., Sunny, A. and Al Ahmed, S.R. (2021) Numerical Investigation on Performance Improvement of WS_2 Thin-Film Solar Cell with Copper Iodide as Hole Transport Layer. *Solar Energy*, **224**, 956-965. https://doi.org/10.1016/j.solener.2021.06.062

[35] Ahmed, S.R.A., Sunny, A. and Rahman, S. (2021) Performance Enhancement of Sb_2Se_3 Solar Cell Using a Back Surface Field Layer: A Numerical Simulation Approach. *Solar Energy Materials and Solar Cells*, **221**, Article ID: 110919. https://doi.org/10.1016/j.solmat.2020.110919

[36] Patel, A.K., Mishra, R. and Soni, S.K. (2022) Performance Enhancement of CIGS Solar Cell with Two Dimensional MoS_2 Hole Transport Layer. *Micro and Nanostructures*, **165**, Article ID: 207195. https://doi.org/10.1016/j.micrna.2022.207195

[37] Fridolin, T.N., Maurel, D.K.G., Ejuh, G.W., Benedicte, T.T. and Marie, N.J. (2019) Highlighting Some Layers Properties in Performances Optimization of CIGSe Based Solar Cells: Case of Cu (In, Ga) Se-ZnS. *Journal of King Saud University-Science*, **31**, 1404-1413. https://doi.org/10.1016/j.jksus.2018.03.026

[38] Boukortt, N.E.I., Patanè, S., Hadri, B. and Crupi, G. (2023) Graded Bandgap Ultrathin CIGS Solar Cells. *Electronics*, **12**, Article 393. https://doi.org/10.3390/electronics12020393